



Thallium isotopic evidence for the Tonian rise and Cryogenian fall of Neoproterozoic oxygen levels

Lucy C. Webb^{1,*}, Francis A. Macdonald², Galen P. Halverson³, Chadlin M. Ostrander⁴, Sune G. Nielsen^{5,6}, and Erik A. Sperling¹

¹Department of Earth and Planetary Sciences, Stanford University, Stanford, California 94305, USA

²Department of Earth and Planetary Science, University of California Berkeley, Berkeley, California 94720, USA

³Department of Earth and Planetary Sciences, McGill University, Montreal, Quebec H3A 0E8, Canada

⁴Department of Geology & Geophysics, University of Utah, Salt Lake City, Utah 84112, USA

⁵Centre de Recherches Pétrographiques et Géochimiques, Université de Lorraine, Nancy 54500, France

⁶Department of Geology & Geophysics, Woods Hole Oceanographic Institution, Woods Hole, Massachusetts 02543, USA

ABSTRACT

Estimating dissolved oxygen (O_2) concentrations in seawater during the Neoproterozoic is central to testing hypotheses about the role of O_2 in animal evolution. Here we apply the thallium (Tl) isotope redox proxy to samples stratigraphically below the ca. 810-million-year-old (Ma) Bitter Springs Carbon Isotope Excursion and spanning the interval between the two Snowball Earth glaciations (ca. 662–650 Ma) to constrain the evolution of Neoproterozoic bottom water redox conditions. Thallium isotopes can be used to reconstruct the global extent of oxygenated oceanic bottom waters because the primary control on seawater Tl isotope compositions ($\varepsilon^{205}\text{Tl}$) over million-year time scales is changes in the amount of ^{205}Tl removal by Mn oxides on the seafloor. Samples spanning an ~20-m.y. period preceding the Bitter Springs excursion from the Tonian Reefal Assemblage ($n = 18/30$) yield $\varepsilon^{205}\text{Tl}_{\text{auth}}$ values lower than global oceanic inputs ($\varepsilon^{205}\text{Tl} \sim -2\text{\textperthousand}$), with some samples approaching the modern seawater $\varepsilon^{205}\text{Tl}$ value of $-6\text{\textperthousand}$. These sustained low $\varepsilon^{205}\text{Tl}_{\text{auth}}$ values require enhanced burial of Mn oxides elsewhere on the seafloor, which we interpret as evidence for the oxygenation of the deep ocean in the Tonian. In contrast, the majority of samples from the Cryogenian Hay Creek Group ($n = 13/16$) yield $\varepsilon^{205}\text{Tl}_{\text{auth}}$ values similar to global oceanic inputs, suggesting that the deep ocean was not ventilated at this time. This indicates that Earth's deep ocean was not gradually oxygenated throughout the Neoproterozoic, but rather experienced intervals of increased and decreased O_2 concentrations.

INTRODUCTION

The amount of O_2 in Earth's atmosphere and oceans throughout geologic time is often portrayed as progressively increasing and invoked as a main control on animal evolution (e.g., Lyons et al., 2014). Molecular clocks and biomarkers suggest that animals may have first appeared during the late Tonian to Cryogenian (Love et al., 2009; Erwin et al., 2011; Dohrmann and Wörheide, 2017). However, O_2 levels remain poorly constrained through this interval, with estimates from $<0.1\%$ to 100% of present atmospheric levels (Cole et al., 2020). Shale Cr isotope ratios that track O_2

concentrations on Earth's surface and shallow marine redox proxies (I/Ca ratios of carbonates and the presence of sulfate evaporites) support increased atmospheric and marine O_2 levels before and during the ca. 810 Ma Bitter Springs Carbon Isotope Excursion (BSE; Cole et al., 2016; Turner and Bekker, 2016; Lu et al., 2017). However, the global marine redox structure and duration of this putative O_2 rise are unclear. Here, we apply the Tl isotope redox proxy, a recently developed tool for reconstructing global-scale changes in bottom water redox conditions, to shales from Tonian and Cryogenian strata in northwest Canada and compare these analyses to published data to test the hypothesis that marine O_2 levels progressively increased throughout the Neoproterozoic.

Lucy C. Webb  <https://orcid.org/0009-0005-4796-0708>
*lcwebb@stanford.edu

CITATION: Webb, L.C., et al., 2026, Thallium isotopic evidence for the Tonian rise and Cryogenian fall of Neoproterozoic oxygen levels: *Geology*, v. XX, p. , <https://doi.org/10.1130/G53625.1>

THALLIUM ISOTOPE PRIMER

Thallium isotopic compositions are reported in epsilon (ε) notation as the ratio of the two stable isotopes of Tl ($^{205}\text{Tl}/^{203}\text{Tl}$) in the sample relative to the U.S. National Institute of Standards and Technology (NIST) 997 Tl standard:

$$\varepsilon^{205}\text{Tl}(\text{\textperthousand}) = \left(\frac{^{205}\text{Tl}_{\text{sample}}}{^{205}\text{Tl}_{\text{NIST-997}}} - 1 \right) \times 10,000. \quad (1)$$

Today, the $\varepsilon^{205}\text{Tl}$ value of seawater is $-6\text{\textperthousand}$ and globally homogeneous because the residence time of Tl (~ 18.5 k.y.) is longer than the mixing time of the ocean (~ 1 k.y.) (Rehkämper et al., 2002; Nielsen et al., 2017; Owens et al., 2017). The $\varepsilon^{205}\text{Tl}$ value of seawater reflects the isotopic balance of one averaged source and three sinks (Nielsen et al., 2017; Owens et al., 2017). The primary sources of Tl to the ocean—subaerial volcanism, rivers, hydrothermal fluids, and dust—can be modeled as a single source because each globally averaged $\varepsilon^{205}\text{Tl}$ value is $\sim -2\text{\textperthousand}$ (Nielsen et al., 2017). The three primary sinks of Tl are low-temperature alteration of oceanic crust, Mn oxide-rich oxic sediments, and sulfide-bearing anoxic sediments. Altered seafloor basalts preferentially remove ^{203}Tl , leading to a $\varepsilon^{205}\text{Tl}$ value for this sink $0\text{--}3\text{\textperthousand}$ lower than seawater (Nielsen et al., 2017). Manganese oxides preferentially remove ^{205}Tl due to the oxidation of Tl(I) to Tl(III) during sorption, leading to an $\varepsilon^{205}\text{Tl}$ value of Mn oxide-rich sediments $10\text{\textperthousand}\text{--}18\text{\textperthousand}$ higher than seawater (Nielsen et al., 2017). The seawater $\varepsilon^{205}\text{Tl}$ value is sensitive to deep ocean oxygenation because sorption of Tl to hydrogenetic hexagonal birnessite, the predominant Mn oxide mineral in slowly accumulating deep-sea sedi-

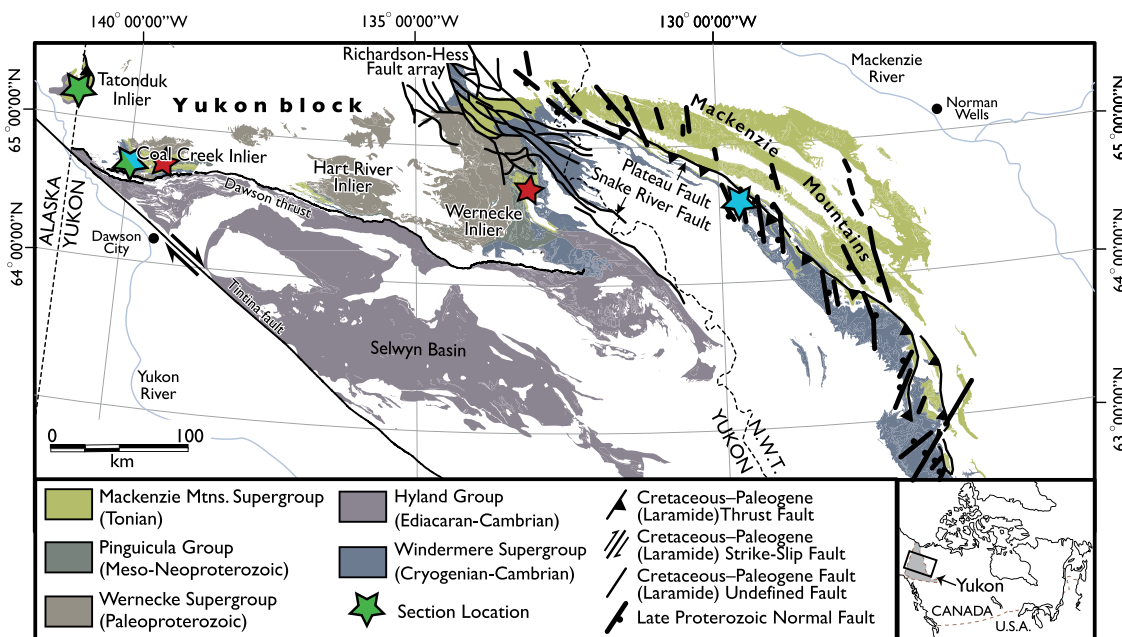


Figure 1. Simplified geologic map of Proterozoic to Paleozoic strata in northwest Canada after Macdonald et al. (2018). Locations of sections from PR1 and the Dolores Creek Formation, the Tonian Fifteenmile Group (Mackenzie Mountains Supergroup), and Cryogenian Hay Creek Group (Windermere Supergroup) are marked with red, green, and blue stars, respectively. N.W.T.—Northwest Territories.

ments, results in the largest fractionation from seawater (Phillips et al., 2023). Stabilization of Mn oxides on the deep seafloor requires the persistent presence of O_2 in overlying bottom waters (Robbins et al., 2023). The $\varepsilon^{205}\text{Ti}$ value of authigenic Ti associated with sulfides ($\varepsilon^{205}\text{Ti}_{\text{auth}}$) in anoxic sediments matches the overlying water column $\varepsilon^{205}\text{Ti}$ value (Owens et al., 2017; Fan et al., 2020). The typical Ti isotope paleoredox proxy approach, which we follow here, is to reconstruct ancient seawater $\varepsilon^{205}\text{Ti}$ values from (unfractionated) fine-grained sediments (“shales”) deposited under locally anoxic conditions and infer from them changes in past seafloor Mn oxide burial occurring elsewhere in the ocean. These changes should scale with global bottom water O_2 availability.

GEOLOGIC BACKGROUND

Fine-grained samples analyzed in this study include shale, siltstone, and lime mudstone from four stratigraphic sections: two from the Reefal Assemblage of the Fifteenmile Group and two from the Hay Creek Group in the Northwest Territories (NWT) and Yukon, Canada (Fig. 1). Reefal Assemblage sections near Mount Harper and Mount Slipper are stratigraphically below a negative carbon isotope excursion interpreted as the BSE (Macdonald et al., 2012; Cohen et al., 2017; Fig. 2). The Mount Harper section samples are stratigraphically below a tuff horizon that yielded a zircon U–Pb age of 811.51 ± 0.25 Ma (Macdonald et al., 2010). The Mount Slipper section precedes and spans the interval that yielded an 810.7 ± 6.3 Ma Re–Os age and contains apatitic scale microfossils (Cohen et al., 2017).

The two Hay Creek Group sections span different time intervals between the Sturtian and Marinoan glaciations in the Cryogenian Period,

suggesting depositional ages between 661 Ma and 639 Ma (Tasistro-Hart et al., 2025; Fig. 3). Section S1404 is at the contact between Sturtian diamictite and the basal Twitya Formation cap carbonate, which elsewhere in the Mackenzie Mountains yielded a 662.4 ± 3.4 Ma Re–Os age (Rooney et al., 2014). Section ES-OT is near the top of the Hay Creek Group in the Ogilvie Mountains. These samples are tentatively assigned an age of ca. 650 Ma due to their position below the Marinoan cap carbonate (Macdonald et al., 2018). Samples from unit PR1 and the Dolores Creek Formation (Meso-proterozoic to early Neoproterozoic) and two samples of the Hay Creek Group from other localities were also analyzed (additional geologic context, geochemical data, and decision tree results available in Table S1 in the Supplemental Material¹).

METHODS

Iron speciation, redox-sensitive trace metal abundances, and total organic carbon (TOC) analyses of these samples were published in Sperling et al. (2013) or generated here following Miller et al. (2017). Samples selected for study include only those likely deposited under locally anoxic conditions and recording seawater $\varepsilon^{205}\text{Ti}$ values (Table S1). Authigenic Ti associated with pyrite was extracted from samples with a 2 M HNO_3 acid leach protocol that avoids detrital Ti (after Owens et al., 2017). Thallium was separated from sample matrix via

two-step ion exchange chromatography and analyzed for its isotopic composition using a Thermo Neptune multi-collector–inductively coupled plasma–mass spectrometer at Woods Hole Oceanographic Institution (after Nielsen et al., 2017; detailed methods in the Supplemental Material).

RESULTS

At Mount Harper, 16 of 18 samples from the ~1700-m-thick Reefal Assemblage have $\varepsilon^{205}\text{Ti}_{\text{auth}}$ values $<-2\text{\textperthousand}$, ranging from $-2.8\text{\textperthousand}$ to $-5.8\text{\textperthousand}$ (Fig. 2A). Two samples from this section with $\varepsilon^{205}\text{Ti}_{\text{auth}}$ values $>-2\text{\textperthousand}$ occur ~350 m below the BSE. At Mount Slipper, $\varepsilon^{205}\text{Ti}_{\text{auth}}$ values near the base of the ~300 m section of the Reefal Assemblage are approximately $-2\text{\textperthousand}$. Up-section, values from $-4.2\text{\textperthousand}$ to $-5.1\text{\textperthousand}$ are recorded (Fig. 2B).

Samples from the base of S1404 within the Sturtian cap carbonate record $\varepsilon^{205}\text{Ti}_{\text{auth}}$ values between $-5.2\text{\textperthousand}$ and $-7.8\text{\textperthousand}$ over ~5 m of stratigraphy (Fig. 3). Up-section within both S1404 and ES-OT, $\varepsilon^{205}\text{Ti}_{\text{auth}}$ values become more positive and range from $-3.1\text{\textperthousand}$ to $-0.2\text{\textperthousand}$. Samples from PR1 (ca. 1460 Ma) and the Dolores Creek Formation (ca. 950 Ma) range from $-2.5\text{\textperthousand}$ to $-3\text{\textperthousand}$ (Fig. 4A).

DISCUSSION

The Meso-Neoproterozoic strata in Yukon and NWT were deposited in large intracratonic basins that likely maintained a connection to the open ocean. The MoEF/UEF ratios (molybdenum enrichment factor to uranium enrichment factor) of samples are consistent with unrestricted to weakly restricted basins like the Cariaco Basin, which today accurately records open-ocean seawater $\varepsilon^{205}\text{Ti}$ (Owens et al., 2017; Fig. S2). Together with Fe-speciation data that

¹Supplemental Material. Detailed sample information, analytical methods, and data tables containing all reported and compiled geochemical data. Please visit <https://doi.org/10.1130/G53625.1/7716942/g53625.pdf> to access the supplemental material; contact editing@geosociety.org with any questions.

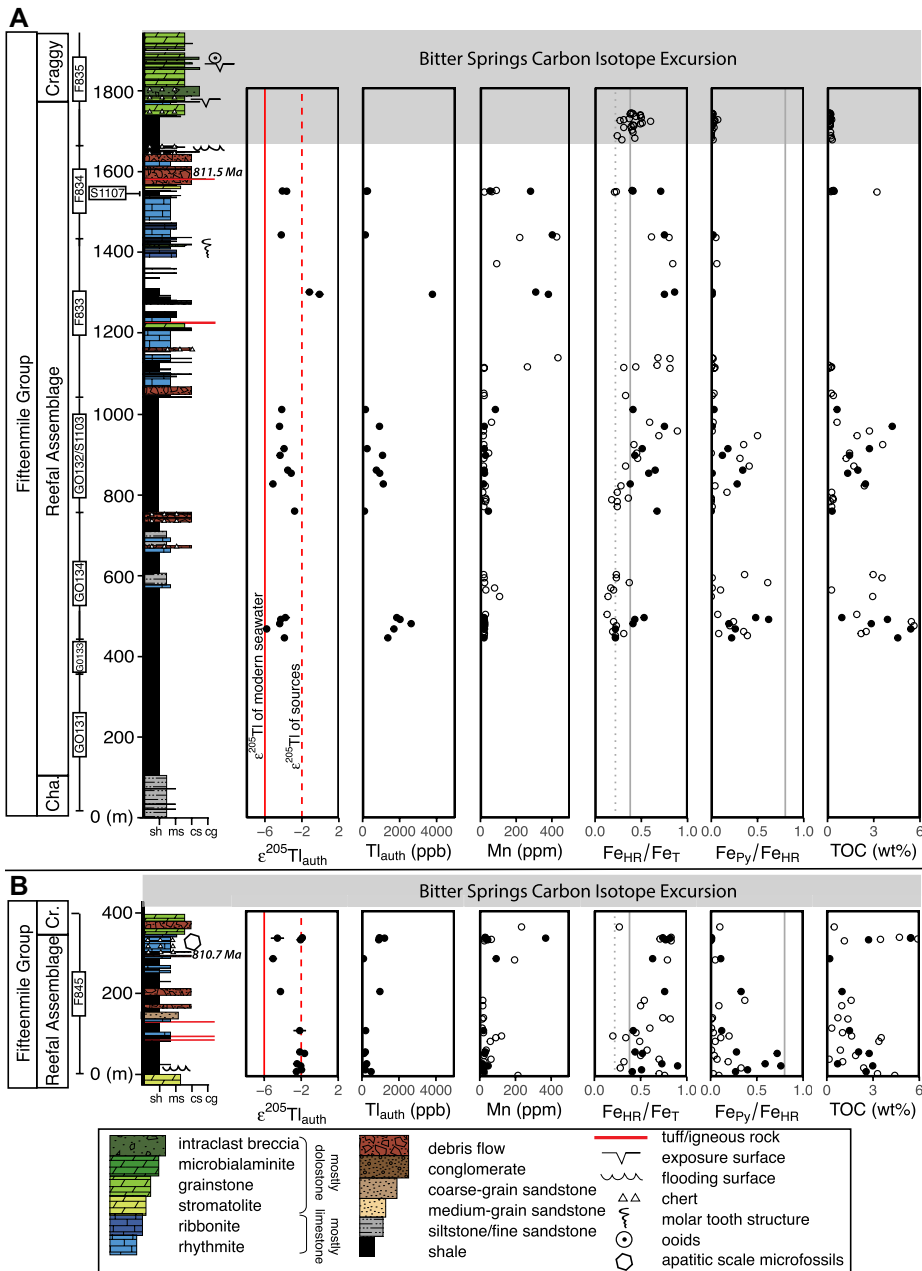


Figure 2. Geochemical data from the Tonian Mount Harper (A) and Mount Slipper (B) sections with stratigraphic columns modified from Sperling et al. (2013). From left to right, the $\varepsilon^{205}\text{Tl}_{\text{auth}}$ values with 2 σ error bars, authigenic Tl concentrations, bulk Mn concentrations, $\text{Fe}_{\text{HR}}/\text{Fe}_T$, $\text{Fe}_{\text{Py}}/\text{Fe}_{\text{HR}}$, and total organic carbon (TOC) contents are plotted against stratigraphic height. Filled points indicate samples analyzed for Tl isotopes. Fe-speciation cutoffs are plotted as vertical lines ($\text{Fe}_{\text{HR}}/\text{Fe}_T = 0.22, 0.38$; $\text{Fe}_{\text{Py}}/\text{Fe}_{\text{HR}} = 0.8$). Cha.—Chandindu; Cr.—Craggy; sh—shale; ms—medium-grained sandstone; cs—coarse-grained sandstone; cg—conglomerate.

indicate locally anoxic bottom waters, variations in the $\varepsilon^{205}\text{Tl}_{\text{auth}}$ values reported here are likely representative of ancient seawater and largely driven by changes in the global extent of seafloor Mn oxide burial. Low seawater $\varepsilon^{205}\text{Tl}$ values require that oxic bottom waters were present over regions of the global seafloor to promote preferential ^{205}Tl removal by Mn oxides, in turn enriching seawater in ^{203}Tl (Fig. 4C). While decreasing the flux of Tl to the alteration of oceanic crust (due to changing seafloor spreading

rates across this long time interval) could result in lower seawater $\varepsilon^{205}\text{Tl}$ values, these changes would not be sufficient to drive values as low as observed here based on the current Tl mass balance (Fig. S4).

Oxygenation of the Deep Ocean versus Shallow Mn Oxide Deposition

Low $\varepsilon^{205}\text{Tl}_{\text{auth}}$ values are interpretable as evidence for oxygenation of the deep ocean because Mn oxides that most strongly frac-

tionate Tl isotopes today form at depths below 1000 m (Wang et al., 2022; Ostrander et al., 2023a, 2025). Manganese oxides are unstable under anoxic conditions, so persistently oxic bottom waters are required for their burial in sediments (Calvert and Pedersen, 1996). These requirements must also be met to promote large Tl isotope fractionation effects (Ostrander et al., 2023b). As seawater depth increases today, so does the Tl isotopic offset between seawater and sedimentary Mn oxides because lower sedimentation rates and reduced organic matter loading enhance Mn oxide stability and accumulation (Wang et al., 2022; Ostrander et al., 2023a).

The locus of seafloor Mn oxide burial may have been closer to shore during some timeframes in Earth's past. For example, the oxidation of a large dissolved Mn(II) reservoir that accumulated in a broadly reducing ocean could have resulted in especially rapid Mn oxide burial over large areas of shallow seafloor (Newby et al., 2021). This mechanism was invoked to explain short-lived low values ($\varepsilon^{205}\text{Tl}_{\text{auth}} = -5.1\text{‰}$) that span ~ 10 m of 2.3 Ga strata and postdate the world's largest sedimentary Mn deposit, the 2.4 Ga Hotazel Formation (Ostrander et al., 2024). This mechanism could result in low $\varepsilon^{205}\text{Tl}_{\text{auth}}$ values without the deep ocean being oxygenated.

In the Tonian, the low $\varepsilon^{205}\text{Tl}_{\text{auth}}$ values are likely driven by the oxygenation of the deep ocean. First, no large sedimentary Mn deposits are known from 850 Ma to 800 Ma (Spinks et al., 2023) that could have temporarily driven seawater $\varepsilon^{205}\text{Tl}$ to low values. The low $\varepsilon^{205}\text{Tl}_{\text{auth}}$ values from the Reefal Assemblage span ~ 1200 m of stratigraphy in the Mount Harper section (Fig. 2A) recording tens of million years of deposition. A large dissolved Mn reservoir likely could not be sustained for that duration since the presumably larger dissolved Mn reservoir in the Paleoproterozoic appears to have been depleted over ~ 10 m of stratigraphy (Ostrander et al., 2024).

Conversely, in the Cryogenian, the relatively short duration of the low $\varepsilon^{205}\text{Tl}_{\text{auth}}$ values in the Sturtian cap carbonate may imply the rapid oxidation of a large dissolved Mn reservoir that developed during the glaciation. The Mn-rich carbonates in the Datangpo Formation in China (and others worldwide; see Spinks et al., 2023) are evidence for large sedimentary Mn deposits at this time (Xiao et al., 2017). The Cryogenian low $\varepsilon^{205}\text{Tl}_{\text{auth}}$ values only span ~ 5 m of stratigraphy (likely < 1 m.y.); the remainder of $\varepsilon^{205}\text{Tl}_{\text{auth}}$ values during this period are comparable to the $\varepsilon^{205}\text{Tl}$ value of averaged Tl sources. Similarly low $\varepsilon^{205}\text{Tl}_{\text{auth}}$ values from and immediately above the Sturtian cap carbonate in the Datangpo Formation support these $\varepsilon^{205}\text{Tl}_{\text{auth}}$ values as representative of seawater at this time (Wang et al., 2025). In summary, the differences

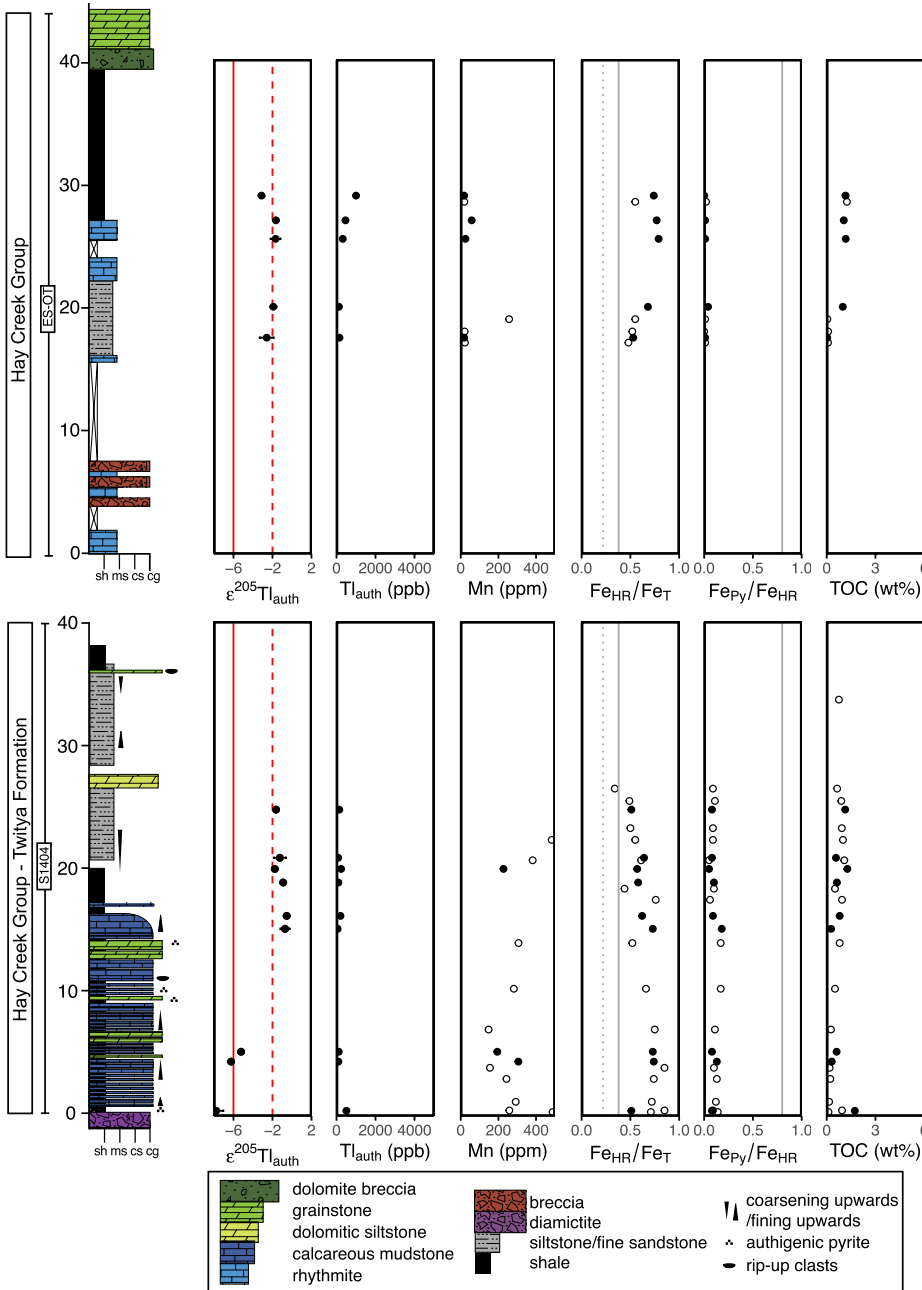


Figure 3. Geochemical data from sections S1404 (bottom) and ES-OT (top) of the Cryogenian Hay Creek Group. Geochemical plots as in Figure 2. TOC—total organic carbon; sh—shale; ms—medium-grained sandstone; cs—coarse-grained sandstone; cg—conglomerate.

in temporal duration and the presence/absence of Mn mineral deposits point to oxygenation of the deep ocean in the Tonian versus the oxidation of a large Mn reservoir without deep ocean oxygenation during deposition of the Sturtian cap carbonate.

Neoproterozoic Redox Evolution

The Tl isotope data presented here are the first to indicate deep ocean oxygenation before the BSE. Other redox proxies also indicate increased oxygenation before and during the BSE, although none track bottom water O_2

(Thomson et al., 2015; Cole et al., 2016; Turner and Bekker, 2016; Lu et al., 2017). Comparing $\varepsilon^{205}\text{Tl}_{\text{auth}}$ values from this study to published data from the Mesoproterozoic to early Paleozoic suggests that the $\varepsilon^{205}\text{Tl}_{\text{auth}}$ values from 850 Ma to 800 Ma are more negative and statistically different from the Cryogenian and Ediacaran (Fig. 4; Table S5). The median $\varepsilon^{205}\text{Tl}_{\text{auth}}$ value from the Reefal Assemblage is $-3.7\text{\textperthousand}$, whereas the median $\varepsilon^{205}\text{Tl}_{\text{auth}}$ value of the Cryogenian and Ediacaran time bins are $-2.5\text{\textperthousand}$ and $-2.3\text{\textperthousand}$. These younger $\varepsilon^{205}\text{Tl}_{\text{auth}}$ values are unfractionated relative to ocean inputs, suggesting limited to no Mn oxide burial on the deep seafloor (Ostrander et al., 2020). The exact timing of Tonian–Cryogenian deep ocean deoxygenation is not clear from these analyses since there are no published $\varepsilon^{205}\text{Tl}_{\text{auth}}$ values from the late Tonian. Other redox proxies including carbonate rare earth element concentrations indicate that late Tonian oceans were anoxic, suggesting that this decrease in marine O_2 availability may have occurred following the BSE (Stacey et al., 2023).

These data suggest that deep marine O_2 availability fluctuated throughout the Neoproterozoic. Models of marine O_2 concentrations throughout the Neoproterozoic that include stable or unidirectionally increasing marine oxygen levels are not supported by these results.

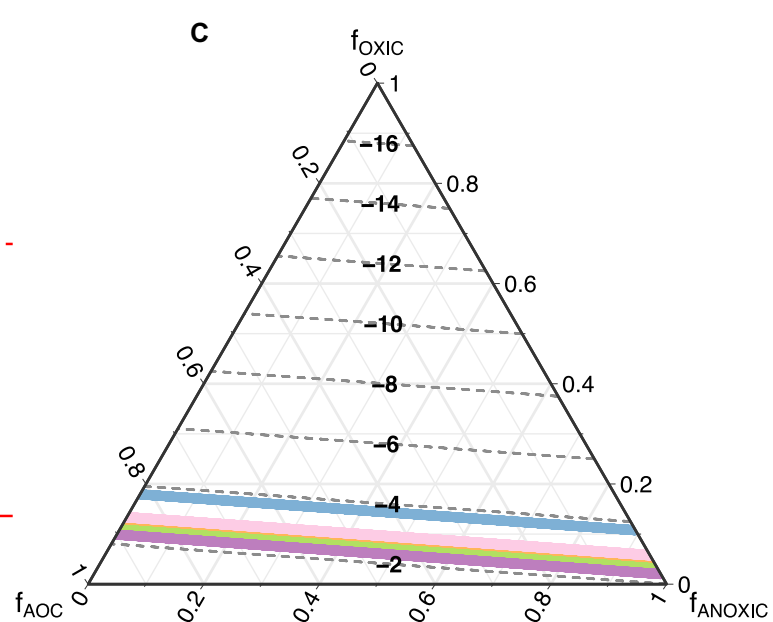
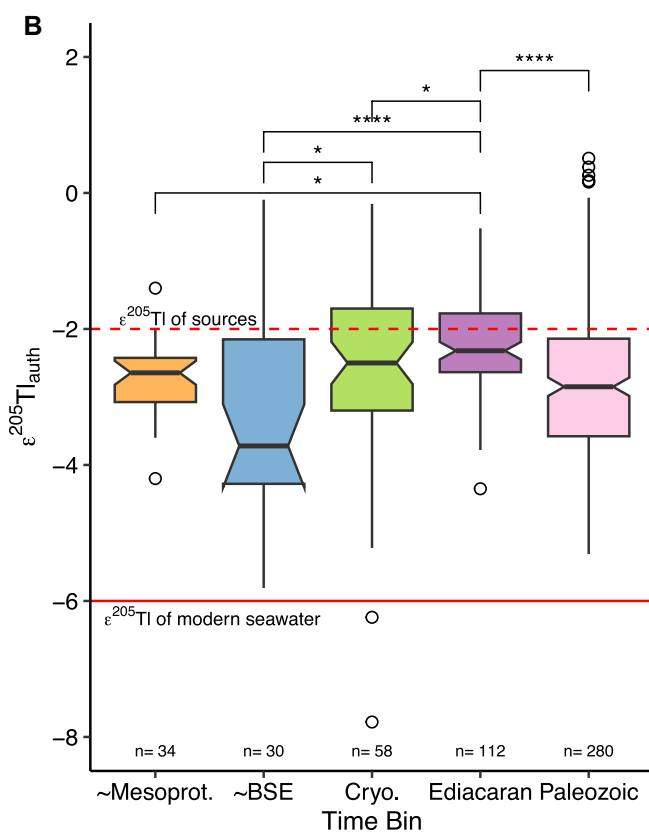
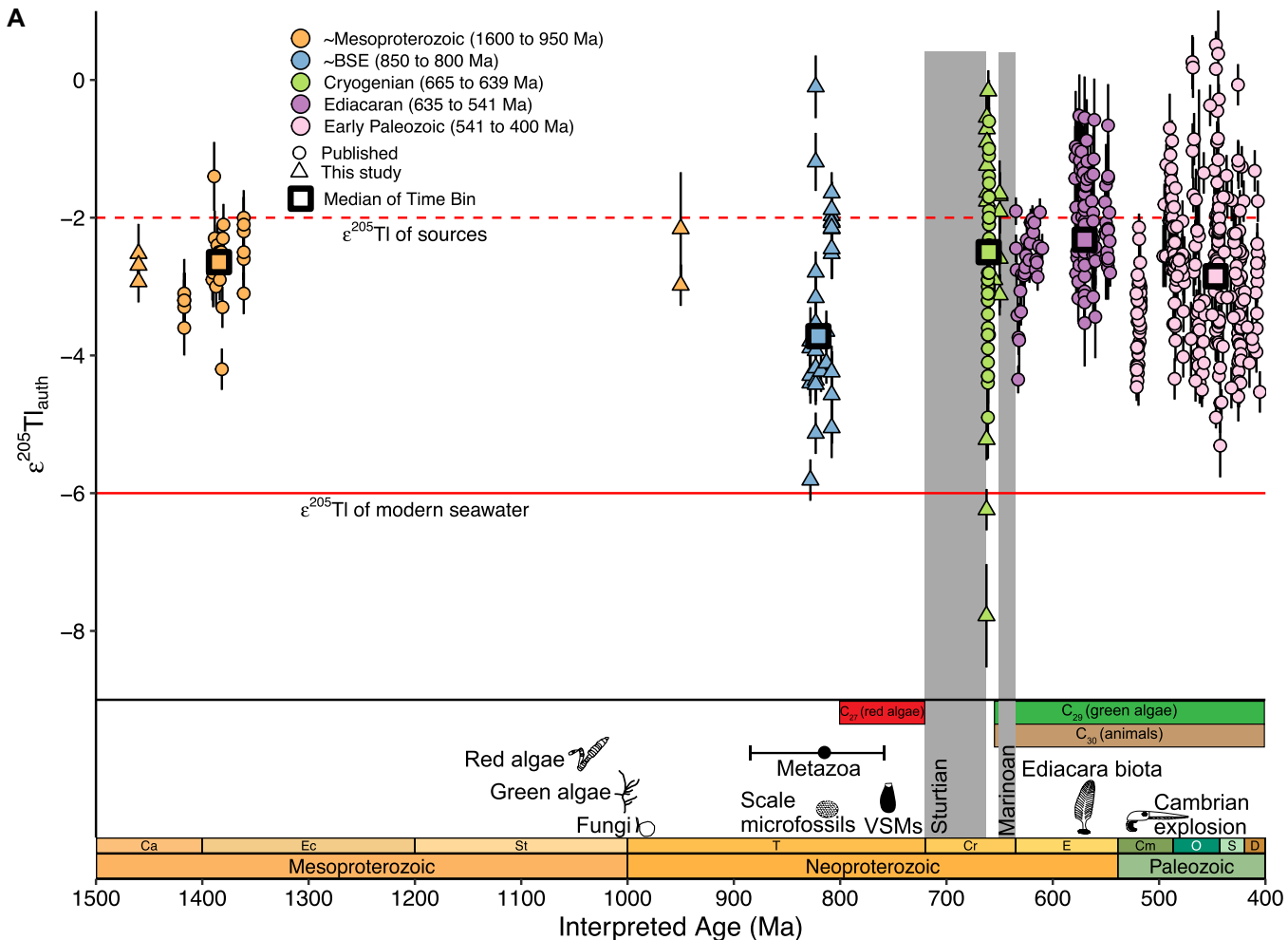
CONCLUSION

This study presents the first $\varepsilon^{205}\text{Tl}_{\text{auth}}$ values from the Tonian and extends the Cryogenian $\varepsilon^{205}\text{Tl}_{\text{auth}}$ record between the Snowball Earth glaciations. Low $\varepsilon^{205}\text{Tl}_{\text{auth}}$ values in the Tonian suggest that the deep ocean was likely oxygenated prior to the BSE. In contrast, with the exception of the excursion in the Sturtian cap carbonate, predominantly crustal $\varepsilon^{205}\text{Tl}_{\text{auth}}$ values from the Cryogenian and Ediacaran suggest that the deep ocean was comparatively anoxic during these periods. Thus, a single or progressive rise in marine O_2 concentrations as proposed in the “Neoproterozoic Oxygenation Event” hypothesis is not supported by these data. Neoproterozoic oceans experienced variable O_2 concentrations with a well-oxygenated ocean during at least parts of the Tonian.

ACKNOWLEDGMENTS

We thank Maureen Auro, Jurek Blusztajn, Yi Wang, Karrie Weaver, and Austin Miller for lab assistance and Justin Strauss, Maxwell Lechte, Katie Maloney, and Charlotte Spruzen for field assistance. We thank the reviewers for their thoughtful reviews that

Figure 4. (A) Compiled $\varepsilon^{205}\text{Tl}_{\text{auth}}$ from the Mesoproterozoic to early Paleozoic (Table S2; see text footnote 1). (B) Distribution of $\varepsilon^{205}\text{Tl}_{\text{auth}}$ across time bins as notched box plots. Pairwise comparisons that are statistically different (Dunn post-hoc test; Benjamini-Hochberg correction) are labeled with asterisks indicating level of significance (Table S5). (C) Ternary diagram of the Tl mass-balance model from Ostrander et al. (2020). Dashed lines represent the seawater $\varepsilon^{205}\text{Tl}$ (bold numbers) that result from the combination of the output fluxes. Medians from each time bin plotted with colors used in panels A and B. AOC—alteration of oceanic crust; BSE—Bitter Springs Carbon Isotope Excursion; VSMs—vase-shaped microfossils; Ca—Calymmian; Ec—Ectasian; St—Stenian; T—Tonian; Cr—Cryogenian; E—Ediacaran; Cm—Cambrian; O—Ordovician; S—Silurian; D—Devonian.



strengthened this manuscript. This manuscript was supported by National Science Foundation awards ECCS-2026822, EAR-1324095, and EAR-2143164, and NASA Exobiology award 80NSSC24K0845.

REFERENCES CITED

Calvert, S.E., and Pedersen, T.F., 1996, Sedimentary geochemistry of manganese: implications for the environment of formation of manganiferous black shales: *Economic Geology*, v. 91, p. 36–47, <https://doi.org/10.2113/gsecongeo.91.1.36>.

Cohen, P.A., Strauss, J.V., Rooney, A.D., Sharma, M., and Tosca, N., 2017, Controlled hydroxyapatite biomineralization in an ~810 million-year-old unicellular eukaryote: *Science Advances*, v. 3, <https://doi.org/10.1126/sciadv.1700095>.

Cole, D.B., Reinhard, C.T., Wang, X., Gueguen, B., Halverson, G.P., Gibson, T., Hodgkiss, M.S., McKenzie, N.R., Lyons, T.W., and Planavsky, N.J., 2016, A shale-hosted Cr isotope record of low atmospheric oxygen during the Proterozoic: *Geology*, v. 44, p. 555–558, <https://doi.org/10.1130/G37787.1>.

Cole, D.B., Mills, D.B., Erwin, D.H., Sperling, E.A., Porter, S.M., Reinhard, C.T., and Planavsky, N.J., 2020, On the co-evolution of surface oxygen levels and animals: *Geobiology*, v. 18, p. 260–281, <https://doi.org/10.1111/gbi.12382>.

Dohrmann, M., and Wörheide, G., 2017, Dating early animal evolution using phylogenomic data: *Scientific Reports*, v. 7, 3599, <https://doi.org/10.1038/s41598-017-03791-w>.

Erwin, D.H., Laflamme, M., Tweedt, S.M., Sperling, E.A., Pisani, D., and Peterson, K.J., 2011, The Cambrian conundrum: Early divergence and later ecological success in the early history of animals: *Science*, v. 334, p. 1091–1097, <https://doi.org/10.1126/science.1206375>.

Fan, H., Nielsen, S.G., Owens, J.D., Auro, M., Shu, Y., Hardisty, D.S., Horner, T.J., Bowman, C.N., Young, S.A., and Wen, H., 2020, Constraining oceanic oxygenation during the Shuram excursion in South China using thallium isotopes: *Geobiology*, v. 18, p. 348–365, <https://doi.org/10.1111/gbi.12379>.

Love, G.D., et al., 2009, Fossil steroids record the appearance of Demospongiae during the Cryogenian period: *Nature*, v. 457, p. 718–721, <https://doi.org/10.1038/nature07673>.

Lu, W., Wörndle, S., Halverson, G.P., Zhou, X., Becker, A., Rainbird, R.H., Hardisty, D.S., Lyons, T.W., and Lu, Z., 2017, Iodine proxy evidence for increased ocean oxygenation during the Bitter Springs Anomaly: *Geochemical Perspectives Letters*, v. 5, p. 53–57, <https://doi.org/10.7185/geochemlet.1746>.

Lyons, T.W., Reinhard, C.T., and Planavsky, N.J., 2014, The rise of oxygen in Earth's early ocean and atmosphere: *Nature*, v. 506, p. 307–315, <https://doi.org/10.1038/nature13068>.

Macdonald, F.A., Schmitz, M.D., Crowley, J.L., Roots, C.F., Jones, D.S., Maloof, A.C., Strauss, J.V., Cohen, P.A., Johnston, D.T., and Schrag, D.P., 2010, Calibrating the Cryogenian: *Science*, v. 327, p. 1241–1243, <https://doi.org/10.1126/science.1183325>.

Macdonald, F.A., Halverson, G.P., Strauss, J.V., Smith, E.F., Cox, G., Sperling, E.A., and Roots, C.F., 2012, Early Neoproterozoic basin formation in Yukon, Canada: Implications for the make-up and break-up of Rodinia: *Geoscience Canada*, v. 39, p. 77–100, <https://journals.lib.unb.ca/index.php/GC/article/view/19397>.

Macdonald, F.A., Schmitz, M.D., Strauss, J.V., Halverson, G.P., Gibson, T.M., Eyster, A., Cox, G., Mamrol, P., and Crowley, J.L., 2018, Cryogenian of Yukon: *Precambrian Research*, v. 319, p. 114–143, <https://doi.org/10.1016/j.precamres.2017.08.015>.

Miller, A.J., Strauss, J.V., Halverson, G.P., Macdonald, F.A., Johnston, D.T., and Sperling, E.A., 2017, Tracking the onset of Phanerozoic-style redox-sensitive trace metal enrichments: New results from basal Ediacaran post-glacial strata in NW Canada: *Chemical Geology*, v. 457, p. 24–37, <https://doi.org/10.1016/j.chemgeo.2017.03.010>.

Newby, S.M., Owens, J.D., Schoepfer, S.D., and Allegre, T.J., 2021, Transient ocean oxygenation at end-Permian mass extinction onset shown by thallium isotopes: *Nature Geoscience*, v. 14, p. 678–683, <https://doi.org/10.1038/s41561-021-00802-4>.

Nielsen, S.G., Rehkämper, M., and Prytulak, J., 2017, Investigation and application of thallium isotope fractionation: *Reviews in Mineralogy and Geochemistry*, v. 82, p. 759–798, <https://doi.org/10.2138/rmg.2017.82.18>.

Ostrander, C.M., et al., 2020, Thallium isotope ratios in shales from South China and northwestern Canada suggest widespread O₂ accumulation in marine bottom waters was an uncommon occurrence during the Ediacaran Period: *Chemical Geology*, v. 557, <https://doi.org/10.1016/j.chemgeo.2020.119856>.

Ostrander, C.M., Bjerrum, C.J., Ahm, A.C., Stenger, S.R., Bergmann, K.D., El-Ghali, M.A.K., Harthi, A.R., Aisri, Z., and Nielsen, S.G., 2023a, Widespread seafloor anoxia during generation of the Ediacaran Shuram carbon isotope excursion: *Geobiology*, v. 21, p. 556–570, <https://doi.org/10.1111/gbi.12557>.

Ostrander, C.M., Nielsen, S.G., Gadol, H.J., Villarroel, L., Wankel, S.D., Horner, T.J., Blusztajn, J., and Hansel, C.M., 2023b, Thallium isotope cycling between waters, particles, and sediments across a redox gradient: *Geochimica et Cosmochimica Acta*, v. 348, p. 397–409, <https://doi.org/10.1016/j.gca.2023.03.028>.

Ostrander, C.M., Heard, A.W., Shu, Y., Bekker, A., Poulton, S.W., Olesen, K.P., and Nielsen, S.G., 2024, Onset of coupled atmosphere-ocean oxygenation 2.3 billion years ago: *Nature*, v. 631, p. 335–339, <https://doi.org/10.1038/s41586-024-07551-5>.

Ostrander, C.M., Clemente, J.N.R., Stockey, R.G., Strauss, J.V., Fraser, T., Nielsen, S.G., and Sperling, E.A., 2025, Dynamic deep marine oxygenation during the Early and Middle Paleozoic: *Science Advances*, v. 11, <https://doi.org/10.1126/sciadv.adw5878>.

Owens, J.D., Nielsen, S.G., Horner, T.J., Ostrander, C.M., and Peterson, L.C., 2017, Thallium-isotopic compositions of euxinic sediments as a proxy for global manganese-oxide burial: *Geochimica et Cosmochimica Acta*, v. 213, p. 291–307, <https://doi.org/10.1016/j.gca.2017.06.041>.

Phillips, R.F., Wang, Y., Klein, F., Farfan, G., Ostrander, C.M., Gadol, H., Hansel, C.M., and Nielsen, S.G., 2023, The role of manganese oxide mineralogy in thallium isotopic fractionation upon sorption: *Geochimica et Cosmochimica Acta*, v. 356, p. 83–92, <https://doi.org/10.1016/j.gca.2023.07.011>.

Rehkämper, M., Frank, M., Hein, J.R., Porcelli, D., Halliday, A., Ingri, J., and Liebetrau, V., 2002, Thallium isotope variations in seawater and hydrogenetic, diagenetic, and hydrothermal ferromanganese deposits: *Earth and Planetary Science Letters*, v. 197, p. 65–81, [https://doi.org/10.1016/S0012-821X\(02\)00462-4](https://doi.org/10.1016/S0012-821X(02)00462-4).

Robbins, L.J., et al., 2023, Manganese oxides, Earth surface oxygenation, and the rise of oxygenic photosynthesis: *Earth-Science Reviews*, v. 239, <https://doi.org/10.1016/j.earscirev.2023.104368>.

Rooney, A.D., Macdonald, F.A., Strauss, J.V., Dudás, F.Ö., Hallmann, C., and Selby, D., 2014, Re-Os geochronology and coupled Os-Sr isotope constraints on the Sturtian snowball Earth: *Proceedings of the National Academy of Sciences of the United States of America*, v. 111, p. 51–56, <https://doi.org/10.1073/pnas.1317266110>.

Sperling, E.A., Halverson, G.P., Knoll, A.H., Macdonald, F.A., and Johnston, D.T., 2013, A basin redox transect at the dawn of animal life: *Earth and Planetary Science Letters*, v. 371–372, p. 143–155, <https://doi.org/10.1016/j.epsl.2013.04.003>.

Spinks, S.C., Sperling, E.A., Thorne, R.L., LaFountain, F., White, A.J.R., Armstrong, J., Woltering, M., and Tyler, I.M., 2023, Mesoproterozoic surface oxygenation accompanied major sedimentary manganese deposition at 1.4 and 1.1 Ga: *Geobiology*, v. 21, p. 28–43, <https://doi.org/10.1111/gbi.12524>.

Stacey, J., Hood, A.S., and Wallace, M.W., 2023, Persistent late Tonian shallow marine anoxia and euxinia: *Precambrian Research*, v. 397, <https://doi.org/10.1016/j.precamres.2023.107207>.

Tasistro-Hart, A.R., Macdonald, F.A., Crowley, J.L., and Schmitz, M.D., 2025, Four-million-year Marinoan snowball shows multiple routes to deglaciation: *Proceedings of the National Academy of Sciences of the United States of America*, v. 122, <https://doi.org/10.1073/pnas.2418281122>.

Thomson, D., Rainbird, R.H., Planavsky, N., Lyons, T.W., and Bekker, A., 2015, Chemostratigraphy of the Shaler Supergroup, Victoria Island, NW Canada: A record of ocean composition prior to the Cryogenian glaciations: *Precambrian Research*, v. 263, p. 232–245, <https://doi.org/10.1016/j.precamres.2015.02.007>.

Turner, E.C., and Bekker, A., 2016, Thick sulfate evaporite accumulations marking a mid-Neoproterozoic oxygenation event (Ten Stone Formation, Northwest Territories, Canada): *Geological Society of America Bulletin*, v. 128, p. 203–222, <https://doi.org/10.1130/B31268.1>.

Wang, L., Cao, M., Lin, Y., Wu, F., Tang, Q., and Zhang, F., 2025, Reconstruction of marine redox landscape during the Cryogenian interglacial oceans using thallium isotopes: *Earth and Planetary Science Letters*, v. 662, <https://doi.org/10.1016/j.epsl.2025.119419>.

Wang, Y., Lu, W., Costa, K.M., and Nielsen, S.G., 2022, Beyond anoxia: Exploring sedimentary thallium isotopes in paleo-redox reconstructions from a new core top collection: *Geochimica et Cosmochimica Acta*, v. 333, p. 347–361, <https://doi.org/10.1016/j.gca.2022.07.022>.

Xiao, J., He, J., Yang, H., and Wu, C., 2017, Comparison between Datangpo-type manganese ores and modern marine ferrromanganese oxyhydroxide precipitates based on rare earth elements: *Ore Geology Reviews*, v. 89, p. 290–308, <https://doi.org/10.1016/j.oregeorev.2017.06.016>.

Printed in the USA